Desalination and Water Treatment
www.deswater.com

doi: 10.5004/dwt.2018.22426

119 (2018) 130–141
July

Evaluation of drift and salt deposition from a natural draft seawater cooling tower. Part I: SACTI analysis

Lianqiang Zhang[a], Zhijie Li[a], Xue Li[a], Yinzhong Wang[a], Jianhua Yin[a,*], Chunhua You[b], Zongzhen Yang[b]

[a]*Institute of Seawater Desalination and Multipurpose Utilization, State Oceanic Administration, Tianjin 300192, China, Tel./Fax: +86 22 87891247; emails: yinjhtj@163.com (J. Yin), 2228208641@qq.com (L. Zhang), lizhijie@tju.edu.cn (Z. Li), xuefenfei1123@163.com (X. Li), 498388455@qq.com (Y. Wang)*
[b]*Suzhou Nuclear Power Research Institute Co. Ltd., Suzhou, China, emails: youchunhua@cgnpc.com.cn (C. You), yangzongzhen@cgnpc.com.cn (Z. Yang)*

Received 7 August 2017; Accepted 14 March 2018

ABSTRACT

Drift and salt deposition from natural draft seawater cooling tower is objectionable for several reasons, especially of the hazards for the environment and equipment. In this work, evaluation of drift and salt deposition from an oversize hyperbolic natural draft seawater cooling tower in closed-cycle cooling system was conducted using SACTI model. The drift droplets have high salt concentration about 1.5–2.0 times original sea water salinity. The data from Weather Research and Forecasting (WRF) model and National Centers for Environmental Prediction (NCEP) were accepted to forecast meteorological parameters. Contour maps of salt deposition of four seasons were drawn according to SACTI results, showing the extent and scope of the effect of salt deposition area of every season. Maximum salt deposition values in spring and summer exceed 10 g/(m^2·month), and potential environmental hazards to the plants and equipment have been forming according to NUREG-1555. Furthermore, comparison of these four maps was made to show salt deposition influence area and trends. The SACTI analytical results provide valuable guidance for further field monitoring study, more field monitoring positions should be set up in severe salt deposition areas for more accurate results.

Keywords: Seawater cooling tower; Natural draft; Drift; Salt deposition; SACTI

1. Introduction

Natural draft cooling tower is a heat rejection device that rejects waste heat to the atmosphere by means of evaporative cooling mostly applied in power generating plant. Water consumption among the heat rejection is through convection between water and air, includes evaporation and water droplets entrained in the air stream known as drift. A large amount of water was consumed every year for cooling process. Seawater has been used since the 1970s in facilities on the coast as a promising method to reduce freshwater consumption. Seawater goes through cooling tower once or recycled, namely once-through cooling and closed-cycle cooling. Once-through cooling requires a significantly greater amount of water than closed-cycle cooling to be withdrawn from a water body, passed once through the power plant to capture waste heat and then discharged back into a water body. Therefore, seawater closed-cycle cooling was recommended by United States Environmental Protection Agency and the California State Water Resources Control Board for its advantages in saving water and protecting marine ecological environment. Recycling seawater in closed-cycle cooling

* Corresponding author.

Presented at 2017 Qingdao International Water Congress, June 27–30, 2017, Qingdao, China.

system usually has 1.5–2.0 times salt concentration of original sea water. Although drift from high salinity seawater cooling tower in closed-cycle cooling system is mostly striped by eliminators, still a little drift discharges from the seawater cooling tower forming salt deposition, contact of these drift salt with plants, building surfaces and human activity can be hazardous [1]. Therefore, special attention must be paid to drift and salt deposition of seawater cooling tower in closed-cycle seawater cooling system. The rate of drift and salt deposition of natural draft seawater cooling tower is related to many factors such as tower configuration, eliminator design, airflow rate and water loading.

In the early investigations, most efforts have been made to understand the operating and thermal characteristics of seawater cooling tower [2–5] and mechanical draft seawater cooling tower drift [6–12], salt deposition of natural draft seawater cooling tower research is few for monitoring difficulty of huge shape and extensive influenced region. In the 1970s, Davis [13] first studied saline drift and vapor emission of natural draft cooling tower using saline river water in Chalk Point electric generating plant (25100 Chalk Point Road Aquasco, Maryland, USA). A numerical model of drift deposition, which was developed and validated against the data collected in the dyed drift experiment at Chalk Point, has been applied to assess the long-term effect on soils, crops and vegetation. The results shows that drift deposition effect on the environment was acceptable. However, their study focused on a saline water cooling tower in once-through cooling system, the drift droplet salinity is less than seawater closed-cycle cooling. Jallouk et al. [14] studied the emission, transport and deposition of drift from the K-31 and K-33 mechanical draft cooling tower at ORGDP. They found that the drift fraction was influenced by drift eliminator and the operating level, the distribution of the deposition flux in the vicinity of the cooling tower is dependent on the temperature gradient between the ambient air at ground level and the air at the same elevation as the top of the cooling tower. Drift and salt deposition from mechanical draft cooling tower is much less than an oversize hyperbolic seawater cooling tower.

Computational fluid dynamics (CFD) techniques constitute a second approach to estimate cooling tower drift and deposition. Meroney [15,16] developed a CFD code to predict natural draft cooling tower plume dispersion and drift, and compared with data from the 1977 Chalk Point Dye Tracer experiment. The validate CFD program was used to predict plume rise, surface concentrations, plume centerline concentrations, surface drift deposition considering the presence of large urban structures. Lucas et al. [17] developed a CFD model to study the influence of psychrometric ambient conditions on cooling tower drift deposition. Both experimental plume performance and drift deposition were employed to validate the numerical results. The results show strongest effect detected corresponds to the ambient dry bulb temperature. Consuegro et al. [18] developed a CFD model of the explosive Legionella's outbreak which took place in 2001 in Murcia, pointing out that CFD method presents a suitable alternative for estimating cooling tower drift, droplet evaporation and deposition. However, most CFD results were validated with the experiment data from Chalk Point Dye Tracer experiment showing a lack of data in the literature. None of these research focus on the closed-cycle seawater cooling system, which has higher salt concentration.

Although CFD simulation has many advantages, it is still in the exploratory stage in drift deposition research. Therefore, many researchers [19–21] studied on the environmental impact of cooling towers focusing on developing an analytical plume prediction model. Policastro et al. [22,23] developed an improved mathematical model, which was well known as the seasonal/annual cooling tower impact (SACTI) model, predicting plume and drift behavior occurring from cooling towers. The SACTI model has been calibrated and validated using an extensive US and European database on cooling tower plumes and drift by Policastro et al. [24] and showed theoretical superiority and better predictive performance. It was recommended by both the United States Environmental Protection Agency (US EPA) and the United States Nuclear Regulatory Commission (US NRC). SACTI model has been an effective method to evaluate environmental impact of the cooling tower before the construction of a new nuclear power plant due to its low cost for the analysis and conservative results for licensing [25].

In this paper, evaluation of drift and salt deposition from an oversize hyperbolic natural draft seawater cooling tower in closed-cycle cooling system which uses high salinity seawater in eastern China was conducted using SACTI model. The tower's configuration is shown in Table 1. SACTI model was conducted considering meteorological and design parameters. Meteorological parameters from Weather Research and Forecasting (WRF) and National Centers for Environmental Prediction (NCEP) were accepted as input meteorological parameters. Contour of salt deposition distribution of four seasons was made using SACTI analytical results to evaluate the influence condition.

2. Research set up

2.1. SACTI model

Steam produced by the heat transfer process of contact between air and seawater on the fill surface, discharge from cooling tower top, was named plume. Plume keeps rising under the interaction of upward momentum and internal energy until plume buoyancy is zero. In addition, plume will diffuse in the horizontal direction with the natural wind. Drift droplet fly along with the plume. SACTI has special plume rise model, including momentum, temperature and humidity layers from inside to outside. As the plume rise up, some surrounding air was mixed with the plume forming a thin layer, maintaining the conservation of flux and saturated

Table 1
SACTI input parameters of seawater cooling tower

Parameter	Value
Fill area (m^2)	13,000
Cooling tower height (m)	177.2
Outlet diameter (m)	79
Heat dissipation rate (MW)	2,404.8
Circulating water Flow (t/h)	100,000
Total air flow rate (kg/s)	30,720
Drifting ratio (%)	0.02
Salt concentration of cooling water (‰)	46

Table 2
Simulation regional grid settings and parameter of WRF

Parameter	Simulation area 1	Simulation area 2	Simulation area 3	Simulation area 4
Horizontal grid distance	27 km	9 km	3 km	1 km
Grid number (east and west, north and south)	(31, 31)	(31, 31)	(31, 31)	(31, 31)
Integral step length of meteorological model	120 s	40 s	13.3 s	4.4 s
Simulation result output time	60 min	60 min	60 min	10 min

conditions including quality, horizontal and vertical momentum, enthalpy and total amount of water. Combined with local meteorological conditions, the shape and distribution of the plume are calculated by solving a series of ordinary differential equations [24].

In this paper, a single source plume rise model [26] was chosen for the research of seawater cooling tower drift. This model assumption was based on geometric structure as shown in Fig. 1. Where, *S* is the distance from the center of projection to the tower. The vertical section of plume variable speed, temperature and humidity properties is assumed constant. As shown in Fig. 2, the plume model consists of three independent radius parameter as the momentum radius R_m, temperature radius *R*, humidity radius R_w. Among them, the temperature radius, *V* is modified by the measured data and the laboratory data. The humidity radius of the plume is modified by field data and the experimental data.

The mass flux Φ_m is given by Eq. (1):

$$\text{Mass flux: } \Phi_m = \pi R_m^2 \overline{\rho_p} V \tag{1}$$

The fractional entrainment rate μ, and entrainment velocity are defined by the following equation:

$$\frac{d\Phi_m}{ds} = \mu\Phi_m \tag{2}$$

$$\mu = \frac{2}{R}\frac{\rho_a}{\overline{\rho_p}}\frac{V_e}{V} \tag{3}$$

This model assumes mass unit around the centerline of the surrounding air has momentum, heat and humidity, and the flux and mass flux according to the following equations to maintain conservation as follows: where Δm is mass unit.

$$\text{Horizontal momentum: } \Phi_{hm} = V_x\Phi_m \tag{4}$$

$$\text{Vertical momentum: } \Phi_{vm} = W\Phi_m \tag{5}$$

$$\text{Enthalpy flux: } \Phi_e = \frac{C_pT_p + \lambda L_v X_p}{v}\Phi_m \tag{6}$$

$$\text{Total water flux: } \Phi_w = \frac{X_p + \sigma}{v}\lambda\Phi_m \tag{7}$$

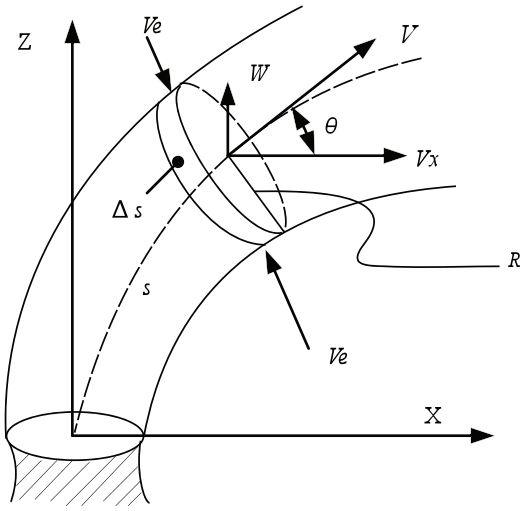

Fig. 1. Structure of plume.

Neither the flux of liquid water nor evaporation water is conserved. However, total water flux is conserved as given by Eq. (8):

$$\Phi_{lw} = \frac{\lambda\sigma}{v}\Phi_m \tag{8}$$

The differential equations of the model are derived from the conservation conditions above, and the lifting process of the plume is obtained by solving the following differential equation of flow function.

$$\frac{d\Phi_m}{ds} = \mu\Phi_m; V_e = \alpha\left|V - U\cos\theta\right| + \beta U\sin\theta \tag{9}$$

$$\frac{d\Phi_{hm}}{ds} = (\mu\Phi_m)U; V_x = U \tag{10}$$

$$\frac{d\Phi_{vm}}{ds} = \Phi_m\frac{g}{\upsilon V}\left(\frac{T_p^* - T_a^*}{T_a^*} - \lambda\sigma\right) \tag{11}$$

$$\frac{d\Phi_e}{ds} = -C_p\frac{W}{\upsilon V}\Phi_m\gamma_d\frac{\rho_a}{\rho_p} + \frac{\mu}{\upsilon}(C_pT_a + \lambda L\upsilon X_a)\Phi_m \tag{12}$$

$$\frac{d\Phi_{tw}}{ds} = \mu\Phi_m\frac{\lambda}{\upsilon}X_a \tag{13}$$

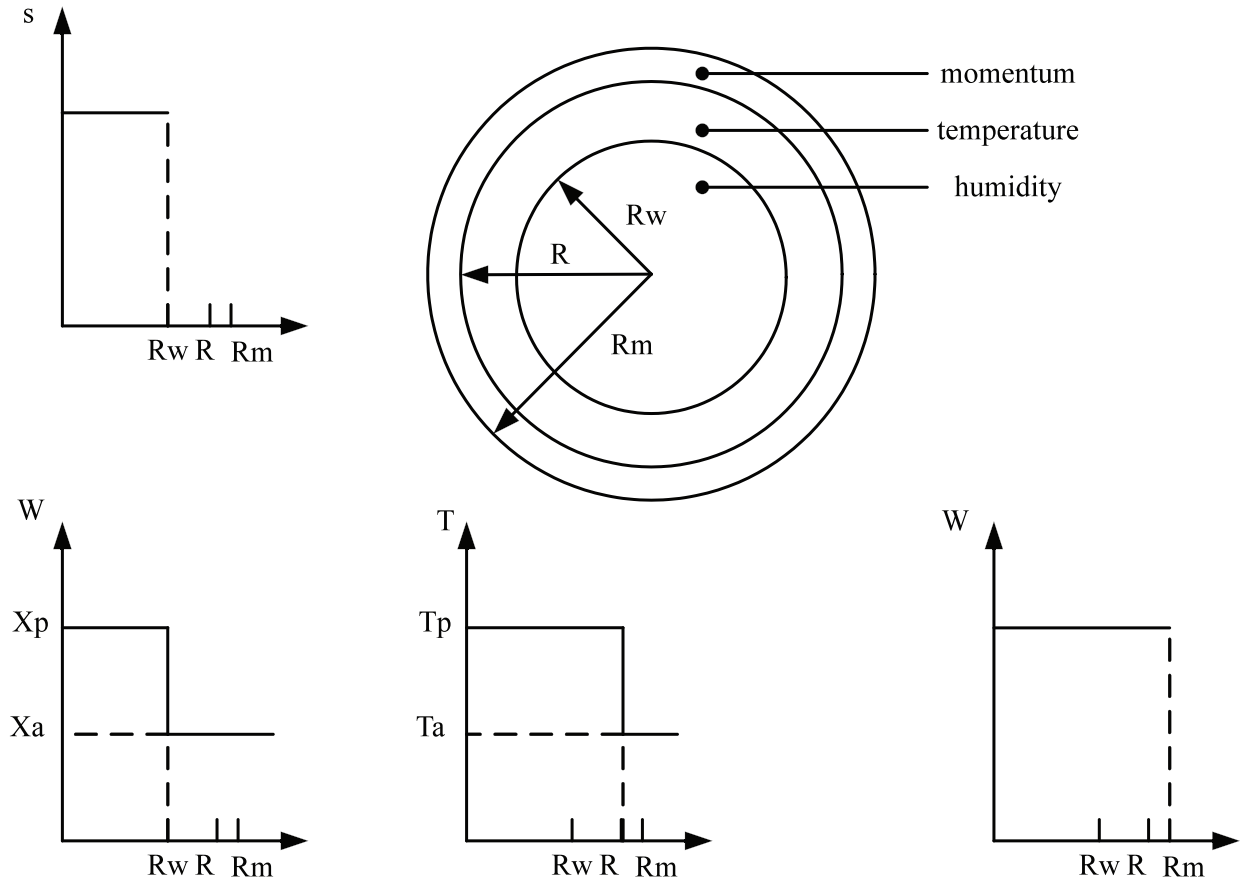

Fig. 2. Cross structure of plume.

$$\frac{d\Phi_{lw}}{ds}=\frac{C_p\Phi_m}{L_v v}\frac{\chi}{1+\chi}\left\{\left(\gamma_d\frac{\rho_a}{\rho_p}+\frac{\Pi}{\tau}\right)\frac{W}{V}+\mu\left[\left(T_p-T_a\right)-\frac{X_p-X_a}{\tau}\right]\right\} \tag{14}$$

$$\frac{dx}{ds}=\frac{U}{V} \tag{15}$$

$$\frac{dz}{ds}=\frac{W}{V} \tag{16}$$

The input data of SACTI include three sections: cooling tower data, meteorological parameters and drift particle size spectrum. The seawater cooling tower input parameters are shown in Table 1. Analytical center coordinate point was set at the center of the two identical seawater cooling tower.

The droplet size spectra measured from a similar oversize hyperbolic natural draft seawater cooling tower in Maryland [13] was adopted for model analysis.

This oversize hyperbolic natural draft seawater cooling tower located in an area of mesoscale mountainous with complex boundary layer as shown in Figs. 3 and 4. Different seasonal weather conditions, typical month of each season such as April (spring), July (summer), October (fall), December (winter) were chosen during calculation process. There is no meteorological observation data in the site of the plant. And the small meteorological observation cannot obtain the complex boundary layer meteorological features.

Considering the great importance of boundary layer of wind, temperature, humidity and other meteorological elements on salt deposition distribution, Weather Research and Forecasting (WRF) and National Centers for Environmental Prediction (NCEP) data were accepted to forecast meteorological parameters.

2.2. WRF model

WRF is a state-of-the-art atmospheric modeling system designed for both meteorological research and numerical weather prediction developed by a collaborative partnership of the National Center for Atmospheric Research (NCAR) and other research institutions. It offers a host of options for atmospheric processes and can run on a variety of computing platforms. The WRF system contains two dynamical solvers, referred to as the ARW (advanced research WRF) core and the NMM (nonhydrostatic mesoscale model) core. In these researches, WRF-ARW was adopted for it contains many physical parameterization schemes which can reasonably parameterize the various physical processes of atmosphere and land. The simulation regional grid settings and parameter of WRF are shown in Table 2. A four-layer nesting scheme is enough to obtain a high-precision meteorological field for the small scale area of this study. Meanwhile, a small amount of observations at the scene with portable observatories was conducted

Fig. 3. Surrounding terrain of cooling tower.

Fig. 4. Cooling tower and surroundings.

for the validation of meteorological parameters model. The long wave and short wave radiation were set as RRTM [27] scheme. Besides, the YSU [28] boundary condition was chosen for planetary boundary layer and land surface model was set as Noah [29]. Kain [30] was used for cumulus parameterization and WSM3 scheme [31] for microphysics. NCEP-FNL reanalysis data, 6 h interval and 1.0° × 1.0° DEG accuracy, was set as initial field and boundary conditions, which was widely used in meteorological research as the best initial condition data of the meteorological model at present. The relaxed boundary was accepted for the side boundary, updated once every 6 h, and the first 12 h of the simulation are considered as the mode adjustment equilibrium stage. The terrain data come from the 30″ resolution USGS, and surface vegetation data were from MODIS with 1 km × 1 km resolution. Fig. 5 shows a case of typical wind fields in the most innermost simulation area of the pattern.

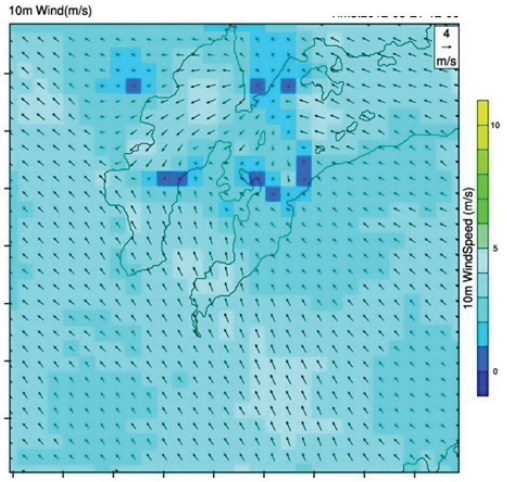

Fig. 5. Typical analytical wind field from WRF.

Finally, the meteorological parameters, including temperature, wet hour data and the atmospheric stability, at 10 m height and the cooling tower top was obtained using WRF model. The dominant direction of the wind rose can be effectively used for analyzing contour values of the environmental assessment indexes as shown in Fig. 6.

3. Results and discussion

3.1. Salt deposition distribution from SACTI model

When the drift droplets come from the top of cooling tower, they were blown away with plume by wind, eventually landing to the ground. Therefore, salt deposition distribution is closely related to wind condition. The distribution of salt deposition around the seawater cooling tower of spring is shown in Fig. 7. The salt deposition distribution gradually decreases from the center of the cooling tower with some serious salt deposition areas in the region. The maximum value of the salt deposition flux is 11.3 g/(m^2 month) with a

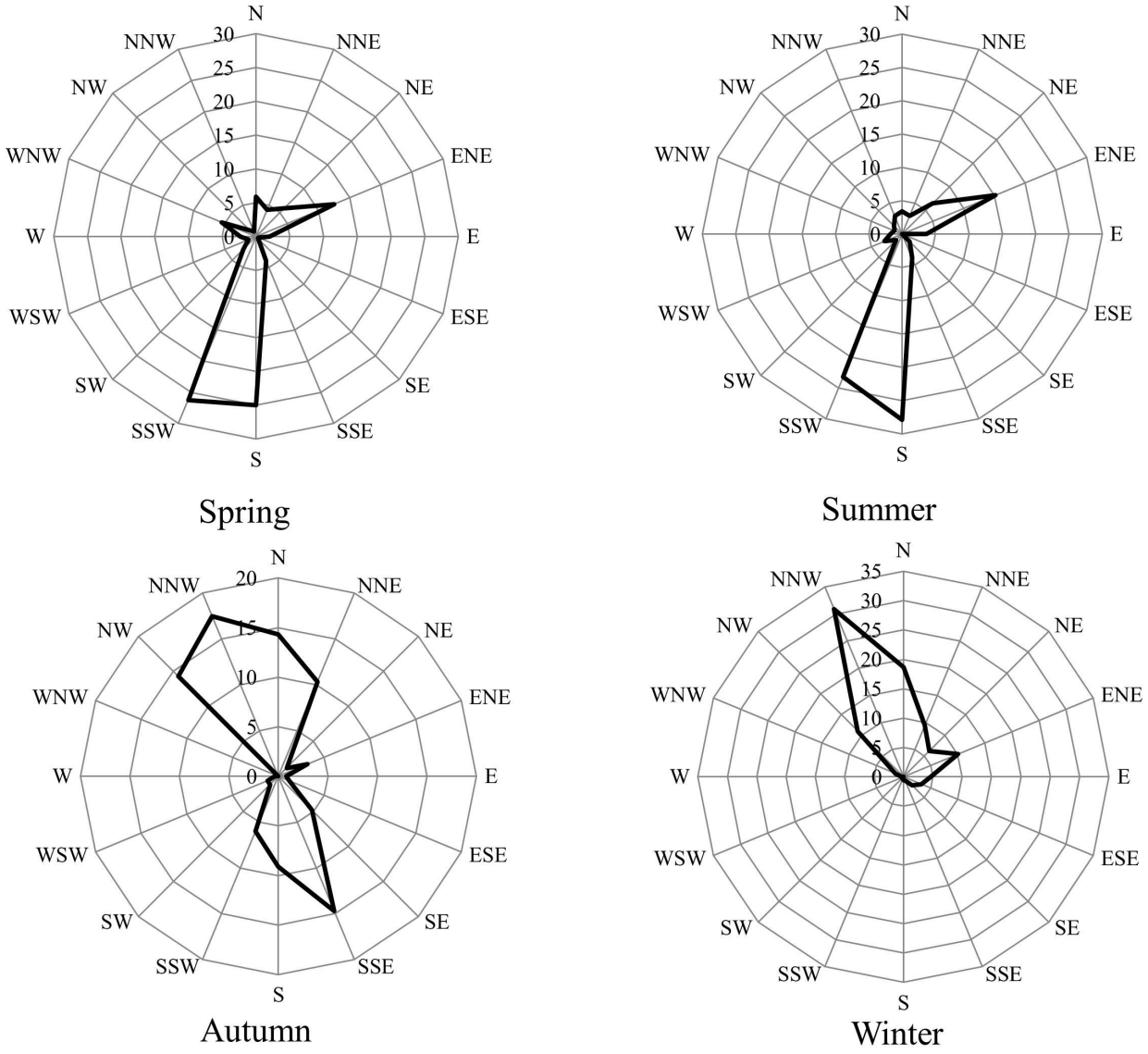

Fig. 6. Wind rose of every 6 h.

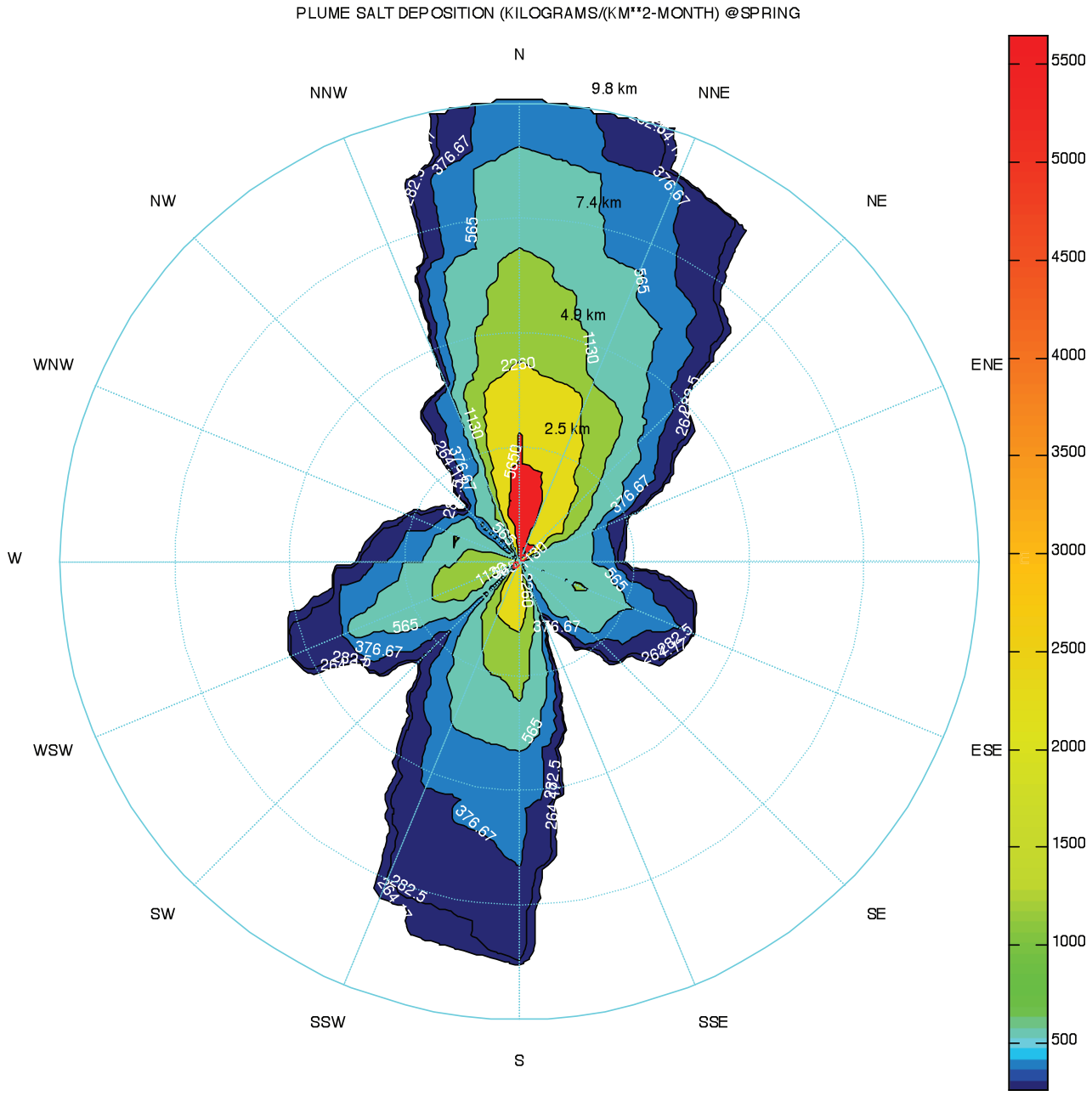

Fig. 7. Analytical salt deposition distribution of spring.

distance of 1,000 m. The severe salt deposition area distributed in north direction along the prevailing wind directions. At this condition, severe salt deposition area concentrating in bar area started from the cooling tower and ended at 2.5 km distance. When the drift exit from the cooling tower top, blowed by the wind, drift droplets gradually fall to the ground in downwind direction with the decrease of the particle diameter. The maximum distance of salt deposition influence is about 10 km.

The distribution of salt deposition around the seawater cooling tower of summer is shown in Fig. 8. There are two high salt deposition areas around the cooling tower in NNE direction and WSW direction. The severe salt deposition bar area in NNE direction also ended about 2.5 km distance similar to spring condition. The other severe salt deposition bar area ended about 1.5 km distance from cooling tower. The severe salt deposition distribution corresponds to the downwind direction. The highest salt deposition value is almost the same as that of spring about 11.2 g/(m^2 month) with a distance of 1 km.

Fig. 9 shows the distribution of salt deposition around the seawater cooling tower of fall. It can be seen that high salt deposition concentration areas mainly concentrated in the NNW direction and S direction, the maximum influence distance is 2.5 km away from the cooling tower. The severe salt deposition bar area is larger than that of spring and summer. Therefore, the average value of severe salt deposition bar area is lower than that of spring and summer. The maximum value of the salt deposition flux is 4.39 g/(m^2 month) with a distance of 400 m.

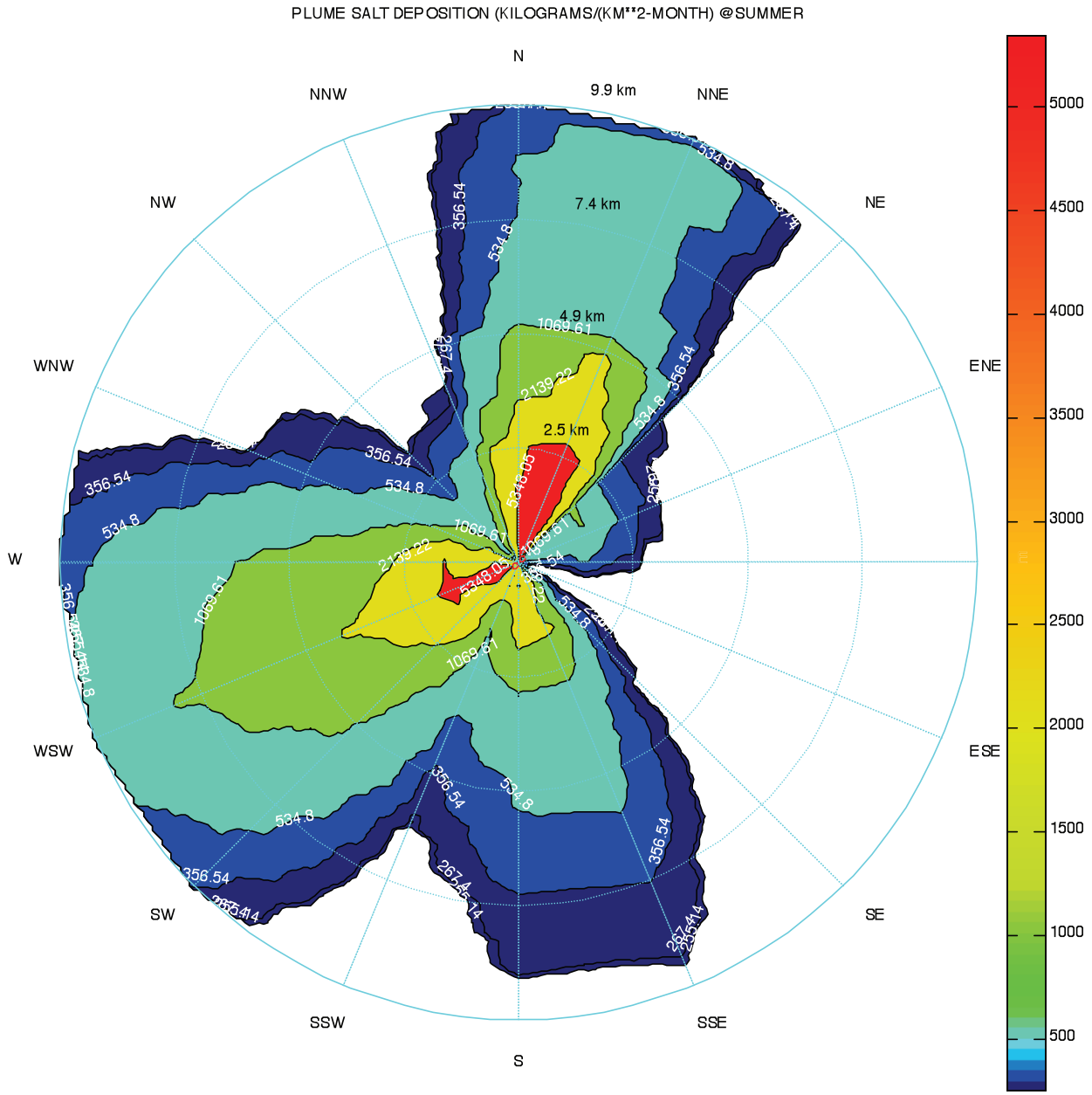

Fig. 8. Analytical salt deposition distribution of summer.

Fig. 10 presents the distribution of salt deposition around the seawater cooling tower of winter. It can be seen that high salt deposition concentration areas mainly concentrated between the S direction and SE direction, the maximum salt deposition position is 1.8 km away from the cooling tower in SSE direction with a value of 6.0 g/(m^2 month). Similar to other season, the maximum distance of salt deposition influence is about 10 km.

3.2. *Comparison of salt deposition distribution of different seasons*

According to analytical result, the distribution of salt deposits is closely related to the wind condition. Severe salt deposition areas are usually in the direction of predominant downwind, presenting a narrowly triangular bar shape with a distance about 2.5 km away from the cooling tower. Moreover, the most serious area of salt deposition concentrates in a circular area with the central 2.5 km radius of the cooling tower for a year. The maximum distance of salt deposition influence is about 10 km of all four seasons. The more wind concentrates, the more severe is the salt deposition, for more drift droplets are blown in an area. According to NUREG-1555 [32]: when salt deposition rate is 0.1–0.2 g/(m^2 month), plant will grow normally; when the salt deposition rate is close to or more than 1 g/(m^2 month), most plant leaves in growing period were hurt; when salt deposition rate is more than 10 g/(m^2 month), with the combine consideration of ecosystem and equipment corrosion, either reduction in salt concentration of circulating water or change in tower design should be done. In this study, salt deposition value in spring and summer exceed 10 g/(m^2 month),

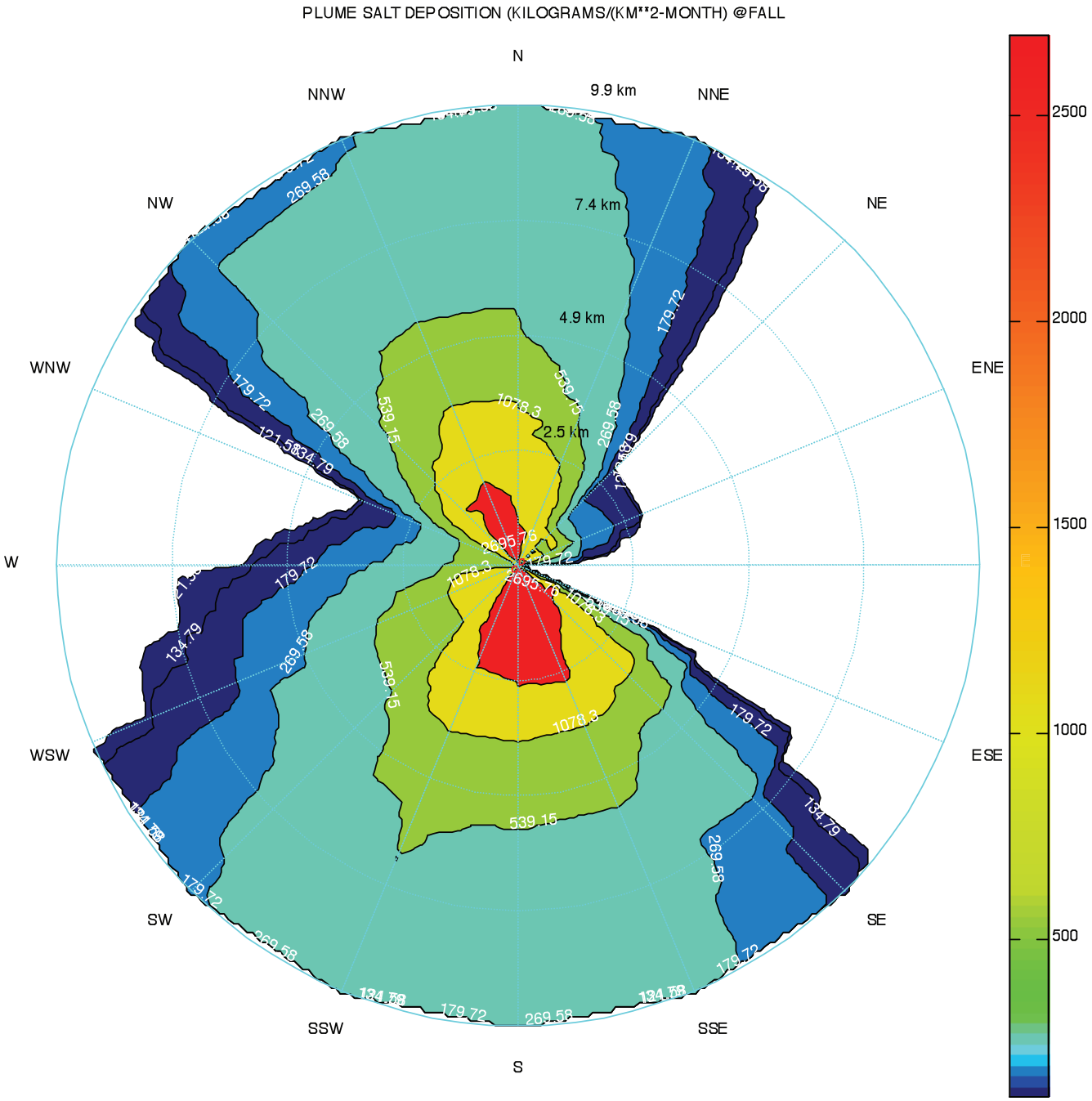

Fig. 9. Analytical salt deposition distribution of fall.

in severe salt deposition area serious harm will form on plant growth. Necessary measures should be taken such as changing efficient eliminator and reducing salt concentration of circulating water to reduce salt deposition. Moreover, the SACTI results show severe salt deposition areas of every season, more monitoring positions should be set at these areas.

4. Conclusion

In this work, salt deposition characteristics of oversize hyperbolic seawater cooling tower was studied by means of SACTI analysis. SACTI model was conducted considering meteorological and design parameters. The data from Weather Research and Forecasting (WRF) and National Centers for Environmental Prediction (NCEP) were accepted as input meteorological parameters. According to SACTI model result, contour maps of salt deposition of four seasons were drawn. Severe salt deposition areas were shown clearly. Comparing these four salt deposition contour maps, the salt deposition is closely related to the wind direction. The maximum salt deposition positions all located in a certain distance of downwind direction, as drift droplet come from the top of cooling tower, they were blown away with plume by wind, eventually landing to the ground. The most serious area of salt deposition

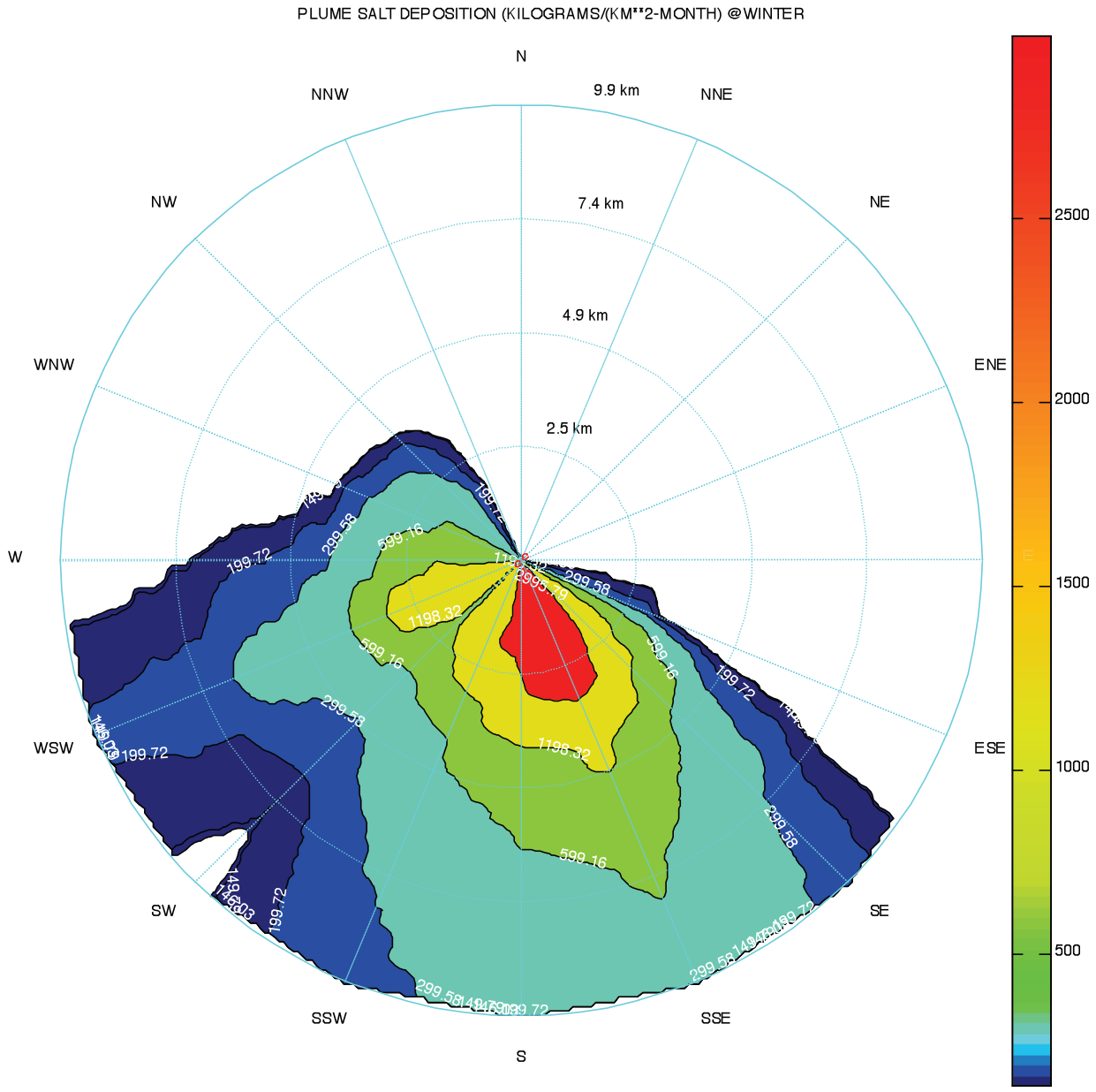

Fig. 10. Analytical salt deposition distribution of winter.

concentrates in a circular area with the central 2.5 km radius of the cooling tower. The more wind concentrates the severe is the salt deposition, for more drift droplets are blown in an area and more monitoring points should be set at the maximum concentration area. In this study, salt deposition value in spring and summer exceed 10 g/(m^2 month) (NUREG-1555), in severe salt deposition area serious harm will form on plant growth. Necessary measures should be taken such as changing efficient eliminator and reducing salt concentration of circulating water reduce salt deposition. The calculation results provide valuable guidance for further application of seawater cooling tower.

Acknowledgments

This research was supported financially by the demonstration project of marine economic innovation and development (BHSF2017-15). And also the research was supported by the Central Level, Scientific Research Institutes for Basic R&D Special Fund Business (K-JBYWF-2016-T5).

Symbols

C_p — Specific heat capacity at constant pressure of dry air, J/kg·°C
g — Acceleration of gravity, m/s^2
k — Crossflow ratio (wind speed at tower top)/(exit velocity)
L_v — Latent heat of evaporation of water, J/kg
Q_s — Saturation mixing ratio at temperature T, pressure P
R_m — Radius of "momentum" plume, m
R_0 — Outlet radius, m
R_w — Radius of "moisture" plume, m

R — Radius of "temperature" plume, m
s — Distance along plume centerline, m
$T_{a,p}$ — Temperature of ambient, plume, K
U — Ambient air velocity, function of z, m/s
V — Total plume velocity, m/s
V_X — Plume horizontal velocity, m/s
V_e — Normal bent-over plume entrainment velocity, m/s
W — Plume vertical velocity, function of s, m/s
$X_{a,p}$ — Mixing ratio of water vapor in ambient, plume, m/s
x — Downwind distance from center of tower exit, m
z — Distance above tower exit, m

Greek

α — First entrainment coefficient
β — Second entrainment coefficient
γ_d — Dry adiabatic lapse rate, °C/m
Θ — Angle of plume centerline with respect to the horizontal
A — Area of moisture core/area of temperature plume
μ — Entrainment rate
υ — Area of momentum plume/area of temperature plume
ρ_a — Ambient air density, kg/m^3
ρ_p — Density of plume air, pointwise, kg/m^3
σ — Liquid water mixing ratio, g/g da
τ — $\tau = \dfrac{\partial Q_s}{\partial T}$
χ — $\chi = \dfrac{\lambda L_v \tau}{C_p}$
Φ_{lw} — Plume liquid water flux, kg/m^2·s
Φ_m — Plume mass flux, kg/m^2·s
Φ_e — Plume enthalpy flux, J/kg·m^2·s
Φ_{tw} — Plume total water flux, kg/m^2·s
Φ_{hm} — Plume horizontal momentum flux, kg/m^2·s
Φ_{vm} — Plume vertical momentum flux, kg/m^2·s

Subscripts

* — Virtual temperatures
p — Plume
a — Ambient

References

[1] J. Shular, R. Barker, B. Nicholson, Locating and Estimating Air Emissions from Sources of Chromium. Supplement, Final report, Midwest Research Institute, Cary, NC, USA, 1989.
[2] M.H. Sharqawy, J.H. Lienhard, S.M. Zubair, On Thermal Performance of Seawater Cooling Towers, J. Eng. Gas Turbines Power, 133 (2011) 649–659.
[3] M.E. Warner, M.R. Lefevre, Salt Water Natural-draft Cooling Tower Design Considerations, Proc. American Power Conference, USA, 1974, p. 36.
[4] Rittenhouse, Salt water cooling tower retrofit experience, Power Eng., 98 (1994) 26–29.
[5] H.U. Jin-Yi, C.Q. Lin, Q.H. Pei, Economic analysis of salt water cooling tower system, Energy Eng., 6 (2011) 64–68.
[6] A. Roffman, L.D.V. Vleck, The state-of-the-art of measuring and predicting cooling tower drift and its deposition, J. Air Waste Manage., 24 (1974) 855–859.
[7] A. Roffman, H. Roffman, Effects of salt water cooling tower drift on water bodies and soil, Water Air Soil Pollut., 2 (1973) 457–471.
[8] G.O. Schrecker, C.D. Henderson, Salt water condenser cooling: measurements of salt water drift from a mechanical-draft wet cooling tower and spray modules, and operating experience with cooling tower materials, Proc. American Power Conference, USA, 1976, p. 38.
[9] G.O. Schrecker, R.O. Webb, D.A. Rutherford, Drift Data Acquired on Mechanical Salt Water Cooling Devices, Final Report, 1975.
[10] Roffman, Predictions of drift deposition from salt water cooling towers, Cooling Tower Institute Publications, Houston, 1973.
[11] M. Gao, N. Wang, Y. Shi, Experimental Research on Environmental Crosswind Effects to Airflow Rate in Wet Cooling Tower, Proc. ASME 2011 Power Conference Collocated with JSME ICOPE, 2011.
[12] J. Ruiz, C.G. Cutillas, A.S. Kaiser, Experimental study of drift deposition from mechanical draft cooling towers in urban environments, Energy Buildings, 125 (2016) 181–195.
[13] E.A. Davis, Environmental Assessment of Chalk Point Cooling Tower Drift and Vapor Emissions, Final report, 1979.
[14] P.A. Jallouk, J.G.J. Kidd, T. Shapiro, Environmental aspects of cooling tower operation: survey of the emission, transport, and deposition of drift from the K-31 and K-33 cooling towers at ORGDP, Report, 1974.
[15] R.N. Meroney, CFD prediction of cooling tower drift, J. Wind Eng. Ind. Aerodyn., 94 (2006) 463–490.
[16] R.N. Meroney, Protocol for CFD prediction of cooling-tower drift in an urban environment, J. Wind Eng. Ind. Aerodyn., 96 (2008) 1789–1804.
[17] M. Lucas, P.J. Martínez, J. Ruiz, On the influence of psychrometric ambient conditions on cooling tower drift deposition, Int. J. Heat Mass Transfer., 53 (2010) 594–604.
[18] A.J. Consuegro, A.S. Kaiser, B. Zamora, A. Viedma, F. Sánchez, M. Hernández, M. Lucas, J. Ruiz, CFD modelling of *Legionella*'s atmospheric dispersion in the explosive outbreak in Murcia, Spain, 38 (2017) 1063–1072.
[19] R.A. Carhart, A.J. Policastro, A second-generation model for cooling tower plume rise and dispersion—I. Single sources, Atmos. Environ. Part A, 25 (1991) 1559–1576.
[20] R.A. Carhart, A.J. Policastro, W.E. Dunn, Improved method for predicting seasonal and annual shadowing from cooling-tower plumes, Atmos. Environ., 26 (1981) 2845–2852.
[21] H.D. Orville, J.H. Hirsch, L.E. May, Application of a cloud model to cooling tower plumes and clouds, J. Appl. Meteorol. Clim., 19 (1980) 1260–1272.
[22] A. Policastro, W. Dunn, R. Carhart, Studies on Mathematical Models for Characterizing Plume and Drift Behavior from Cooling Towers, Executive Summary, 1981.
[23] A.J. Policastro, L. Coke, M. Wastag, User's Manual: Cooling-Tower-Plume Prediction Code, Ai Memo N, 1984.
[24] A.J. Policastro, W.E. Dunn, R.A. Carhart, A model for seasonal and annual cooling tower impacts, Atmos. Environ., 28 (1994) 379–395.
[25] J. Lee, Evaluation of impacts of cooling tower design properties on the near-field environment, Nucl. Eng. Des., 326 (2018) 65–78.
[26] W.E. Dunn, P. Gavin, B. Boughton, Studies on Mathematical Models for Characterizing Plume and Drift Behavior from Cooling Towers, Vol. 3, Mathematical Model for Single-source (Single-tower) Cooling Tower Drift Dispersion, 1981.
[27] E.J. Mlawer, S.J. Taubman, P.D. Brown, Radiative transfer for inhomogeneous atmospheres: RRTM, a validated correlated-k model for the longwave, J. Geophys. Res., 102 (1997) 16663–16682.
[28] S.Y. Hong, Y. Noh, J. Dudhia, A New Vertical Diffusion Package with an Explicit Treatment of Entrainment Processes, Mon. Weather Rev., 134 (2006) 2318.
[29] F. Chen, J. Dudhia, Coupling an Advanced Land Surface Hydrology Model with the Penn State NCAR MM5 Modeling System, Part I: Model Implementation and Sensitivity, Mon. Weather Rev., 129 (2001) 569–585.
[30] J.S. Kain, The Kain Fritsch convective parameterization: an update, J. Appl. Meteorol. Clim., 43 (2004) 170–181.

[31] S.Y. Hong, J. Dudhia, S.H. Chen, A Revised approach to ice microphysical processes for the bulk parameterization of clouds and precipitation, Mon. Weather Rev., 132 (2004) 103–120.

[32] Office of Nuclear Reactor Regulation, Standard Review Plans for Environmental Reviews for Nuclear Power Plants: Environmental Standard Review Plan(NUREG-1555), 2013.